Cellular and Molecular Bioengineering (© 2012)
DOI: 10.1007/s12195-012-0229-8

BMES BIOMEDICAL ENGINEERING SOCIETY™ www.bmes.org

Perturbations in Microtubule Mechanics from Tubulin Preparation

TAVIARE L. HAWKINS,[1] MATTHEW MIRIGIAN,[2] JINGQIANG LI,[3] M. SELCUK YASAR,[1] DAN L. SACKETT,[2] DAVID SEPT,[4] and JENNIFER L. ROSS[1]

[1]Department of Physics, University of Massachusetts Amherst, 666 North Pleasant Street, 302 Hasbrouck Lab, Amherst, MA 01003, USA; [2]National Institutes of Health, Bethesda, MD 20892, USA; [3]Department of Physics, Zhejiang University, Hangzhou, Zhejiang Province, People's Republic of China; and [4]Department of Biomedical Engineering and Center for Computational Medicine and Bioinformatics, University of Michigan, Ann Arbor, MI 48109, USA

(Received 19 November 2011; accepted 7 April 2012)

Associate Editor William O. Hancock oversaw the review of this article.

Abstract—Microtubules are essential structures for cellular organization. They support neuronal processes and cilia, they are the scaffolds for the mitotic spindle, and they are the tracks for intracellular transport that actively organizes material and information within the cell. The mechanical properties of microtubules have been studied for almost 30 years, yet the results from different groups are startlingly disparate, ranging over an order of magnitude. Here we present results demonstrating the effects of purification, associated-protein content, age, and fluorescent labeling on the measured persistence length using the freely fluctuating filament method. We find that small percentages ($<1\%$) of residual microtubule-associated proteins left over in the preparation can cause the persistence length to double, and that these proteins also affect the persistence length over time. Interestingly, we find that the fraction of labeled tubulin dimers does not affect the measured persistence length. Further, we have enhanced the analysis method established by previous groups. We have added a bootstrapping with resampling analysis to estimate the error in the variance data used to determine the persistence length. Thus, we are able to perform a weighted fit to the data to more accurately determine the persistence length.

Keywords—Flexural rigidity, Bending stiffness, Cytoskeletal network.

INTRODUCTION

Microtubules are non-covalent polymer tubes made from tubulin protein hetero-dimers.[8] They are essential to a number of vital cellular processes including intracellular transport, mitosis, and cell morphology. Microtubules have a large impact on the interior organization of the cell, and this organization depends on their ability to be long, straight, rigid rods. Further, several recent engineering studies have begun to use microtubules as scaffolding for nano-scale endeavors.[3,14] Some have proposed to use them as drug-delivery shuttles with their open lumens loaded with the drug of choice. Microtubules can then be inserted into the cell, and the drugs can be slowly released over time.[32] Microtubules have been demonstrated to be molecular shuttles that can be propelled on a bed of motor proteins and directed with magnetic fields.[7,16,17,24] Thus, the rigidity of microtubule filaments is an important question for basic biology, biomedical engineering, and nanoscience disciplines.

Microtubule rigidity has been studied for almost 30 years by a variety of biophysical methods (for a review, see Hawkins *et al.*[15]). Previous measurements of microtubule persistence length show large variability and inconsistency in the literature.[15] Even studies of the same parameters and method performed by different groups can have discrepancies of up to an order of magnitude (0.5–5 mm).[15] Further, measurements in the same study have a large deviation in the resulting persistence lengths (see for instance Brangwynne *et al.*[2] and Gittes[13]), making it difficult to perform accurate statistics to compare between different experimental parameters. These discrepancies could arise from differences in tubulin source and preparation, tubulin isotype, post-translational modifications, purification and storage, labeling, and the presence and type of contaminating microtubule-associated proteins.

To add to the confusion, two studies have reported that microtubules have a persistence length that depends on the contour length.[21,28] These experiments used similar experimental systems, but one found the effect only in the absence of the chemotherapeutic drug Taxol,[20,21] while the other had Taxol present.[28] This is

Address correspondence to Jennifer L. Ross, Department of Physics, University of Massachusetts Amherst, 666 North Pleasant Street, 302 Hasbrouck Lab, Amherst, MA 01003, USA. Electronic mail: rossj@physics.umass.edu

Published online: 25 April 2012

contrary to polymer theory and continuum mechanics, which assumes that the mechanical properties of a material do not depend on the amount of the material present. If these studies are correct, it implies that the mechanics of short microtubules are not governed by continuum mechanics, and the inter-dimer bonding is important.[34]

Using the thermal fluctuation method with a bootstrapping analysis, we compared the effects of several parameters: preparation purity, age of stable microtubules, and labeling. Many studies take for granted that the persistence length will not change much with these variables. Here, we report that preparation and age can affect the persistence length measurement by a factor of 2, but that labeling does not. Further, we are able to see clear differences by comparing the normal distributions of persistence length measurements after natural-log transforming the data. The ability to use normal distributions gives more statistical strength to the differences we find.

EXPERIMENTAL METHODS

Fluctuating Filament Method

The most frequently used technique to study filament mechanics was established independently by two groups.[13,26] This technique uses observations of thermally induced fluctuations in the filament shape, and have been used extensively.[2,4,13,15,19,21,23,27] The filament is imaged, typically in fluorescence, and the image is segmented for analysis. For the freely fluctuating methods, the shape is approximated by Fourier mode decomposition into sines or cosines. The persistence length is inversely proportional to the variance of the mode amplitudes. For long-wavelength modes ($n < 5$), the signal of the filament shape is typically much larger than the noise, but for higher modes, the noise dominates because the shot and thermal noise of the video microscopy technique has fluctuations on the same spatial wavelength (Eq. (1)).[13] Gittes derived a now well-used formula that takes into account that the noise floor rises at high mode numbers:

$$\mathrm{var}(a_n) = \left(\frac{L_c}{n\pi}\right)^2 \frac{1}{L_p} + \frac{4}{L_c}\left\langle \varepsilon_k^2 \right\rangle \left[1 + (N-1)\sin^2\left(\frac{n\pi}{2N}\right)\right] \tag{1}$$

where, $\mathrm{var}(a_n)$ is the variance nth mode amplitude, a, measured from the data, L_c is the contour length of the filament, and N is the number of segments taken along the microtubule to describe its shape.[13] The fitting parameters L_p and $\langle \varepsilon_k^2 \rangle$ are the persistence length and the average of the error due to noise in the position squared, respectively.

Previous studies have only fit the first few modes, with low noise, to a form where the variance is inversely proportional to the persistence length, without the noise term[2,13]:

$$\mathrm{var}(a_n) = \left(\frac{L_c}{n\pi}\right)^2 \frac{1}{L_p} \tag{2}$$

Others have used Eq. (2) to directly calculate L_p for the first few modes and then average them together.[19] In order to increase the accuracy of our measurements, we wanted to determine the error in the variance estimate. Directly doing this would require multiple measurements on the same microtubule, but such experiments are difficult since the fluorescence signal and the microtubule itself both degrade with prolonged exposure to light.[2,13] Instead, we implemented the bootstrap method to resample each data set giving us the variance as well as its standard error, where the error can be used to perform a weighted fitting to Eq. (1).

Reagents and Experimental Procedures

Unless otherwise stated, all reagents were purchased from Sigma. Tubulin was either purchased from a commercial vendor (Cytoskeleton, Denver, CO) or made in-house. Commercial tubulin from porcine brains that was unlabeled (Cytoskeleton catalogue #TL238, lot #053) or labeled with tetramethylrhodamine to a ratio of 1–2 rhodamine dyes per dimer (Cytoskeleton catalogue #TL590M, lots #003 and #013) were both delivered lyophilized and stored at −80 °C until use. Cytoskeleton tubulin is made by three cycles of polymerization and depolymerization followed by a phosphocellulose (PC) column to remove excess MAPs, as described.[33] All rhodamine tubulin was purchased and not made in-house.

In-house tubulin was purified as previously described.[29] Briefly, three pig brains were homogenized in PEM-100 (100 mM PIPES, pH 6.8 with KOH, 2 mM EGTA, and 1 mM $MgSO_4$) and centrifuged to retain the supernatant with soluble tubulin proteins. Tubulin was purified from the supernatant by polymerization at 37 °C by adding an equal volume of GPEM-76 [8 M Glycerol (58% vol:vol), 76 mM PIPES, 2 mM EGTA, 1 mM $MgSO_4$] with 1 mM Guanosine Triphosphate (GTP). The microtubules were pelleted at 300,000×g at 37 °C for 45 min, and the supernatant was removed. Pellets were resuspended at 4 °C by homogenization to depolymerize microtubules. This completed one cycle of polymerization and depolymerization that was repeated two more times. After three cycles, a fourth cycle was performed in the presence of 1 M PIPES to remove the remaining

MAPs. Aliquots of 10 mg/mL tubulin were drop frozen in liquid nitrogen and stored at −80 °C until used. We will refer to our in-house tubulin as "in-house" throughout the text to distinguish it from the "commercial" tubulin.

Lyophilized tubulin (unlabeled or rhodamine-labeled) was hydrated in PEM-100 to 5 mg/mL without GTP and allowed to resuspend for 10 min at 4 °C. Rhodamine tubulin was mixed with unlabeled tubulin to desired ratio (7, 10, 16, or 25%). Tubulin was centrifuged at 298,000×g at 4 °C to remove any aggregated tubulin. GTP was added to 1 mM to the supernatant and incubated at 37 °C for 20 min to polymerize microtubules. Paclitaxel (Taxol) was added to 50 μM to stabilize microtubules. Microtubules were incubated at 37 °C for 20 min to equilibrate the Taxol. Microtubules were centrifuged at 14,000×g for 10 min at 25 °C to remove any unpolymerized tubulin, and the pellet was resuspended in PEM-100 with 50 μM Taxol, but without GTP. We added 7.65 mM Sodium Azide to prevent bacterial growth. The microtubules were stored at 37 °C.

Slides and cover glass (Fisher 1.5 cat #CO406) were cleaned by 70% ethanol and dried with Kimwipes. Slides and cover glass were coated with Kappa-Casein (10 mg/mL in PEM-100) by pipetting a 10 μl drop of casein onto Parafilm and placing the slide or cover glass onto the drop so that it spread over the entire cover glass surface. Casein blocks the glass to prevent microtubules from adhering. The slide and cover glass were allowed to air dry under a Petri dish to keep free of dust.

Microtubules were diluted to 0.05 mg/mL in PEM-100 with 50 μM Taxol, and an oxygen scavenger system (0.45 mg/mL glucose oxidase, 0.134 mg/mL catalase, and 13.6 mg/mL glucose) was added to prevent photobleaching and damage. We dropped 0.85 μL of microtubule dilution on the slide, and placed the cover glass on top with the casein-coated sides facing the inside of the sample. Samples were firmly pressed to ensure the microtubule sample spread throughout the entire cover glass area. A Kimwipe was used to wick excess sample from the edges while pressing. Chambers were sealed on all four sides using a thin layer of epoxy that was allowed to fully dry before imaging.

Chamber thickness was determined by the calibrated microscope focus noting the height between the top and bottom of the chamber. The difference between the heights gave the thickness of the sample, which had to be ≤3 μM to be used in the assay. Microtubules were imaged in epi-fluorescence using a Nikon TiE scope with Intenselite illumination, a 60×, 1.49 NA objective with a 2.5× image expander (Nikon) in front of the Cascade II EM-CDD camera (Roper) cooled to −80 °C. Images were captured to RAM with no delay with a 100 ms exposure time interval for 1000 frames. Microtubules chosen for imaging needed to be well separated from all other filaments, freely fluctuating, and confined within one focal plane. A 2:1 signal to noise ratio of fluorescence images above background was required for analysis. Data were recorded as nd2 files using NIS Elements (Nikon) and exported as 16-bit gray scale tiff files.

Data Analysis

Data of fluctuating filaments were analyzed using MATLAB code. Prior to analysis in MATLAB, the images of the microtubules were cropped and rotated using NIS Elements. The images were cropped to remove other filaments and to reduce processing time. The images were rotated so that the microtubules were close to horizontal for analysis, since vertical filaments would cause two values of y for a single x-value, which would be difficult to fit to a function in the MATLAB code.

Our MATLAB code read the cropped tiff files, thresholded the images to black and white, dilated the images to fill holes, and skeletonized each image of the filament. Skeletonized images that still had holes or had significant length changes (>10%) were discarded and not included in the analysis. The microtubule was segmented into 23–25 equally spaced segments that defined the position of the filament in either x–y coordinates or in distance along the filament, s, and angle between the s and $s + 1$ segment is θ_s.[13]

Next, the MATLAB code used the filament position to determine the Fourier mode amplitudes for each image for the first 25 modes (a_n, $1 < n < 25$), as previously described.[2,13] The data were analyzed further using either the previously established method by Gittes, which we call "Prior", or the new bootstrap method we present here.

The MATLAB code calculated the variance of the amplitude for each mode over the entire data set of 1000 frames. The data were plotted over the mode number, to determine which modes were dominated by the noise regime. The first 2–4 modes were fit with Eq. (2) to find the persistence length L_p, as reported previously,[2,13,23] and the fitting error was quoted as the error in L_p (Fig. 1c, black fit curve). Alternatively, Eq. (2) was used to individually calculate L_p for each of the modes 2–5. These values of L_p were averaged and the standard deviation was taken as the error in the measurement, as previously reported.[19] These two methods revealed similar results for the persistence length and were implemented as the "Prior" method. The error due to noise was calculated by fitting the final 5–25 modes to the second term of the sum in Eq. (1) to determine, and the error in the fit was used for the error value of $\langle \varepsilon_k^2 \rangle$.

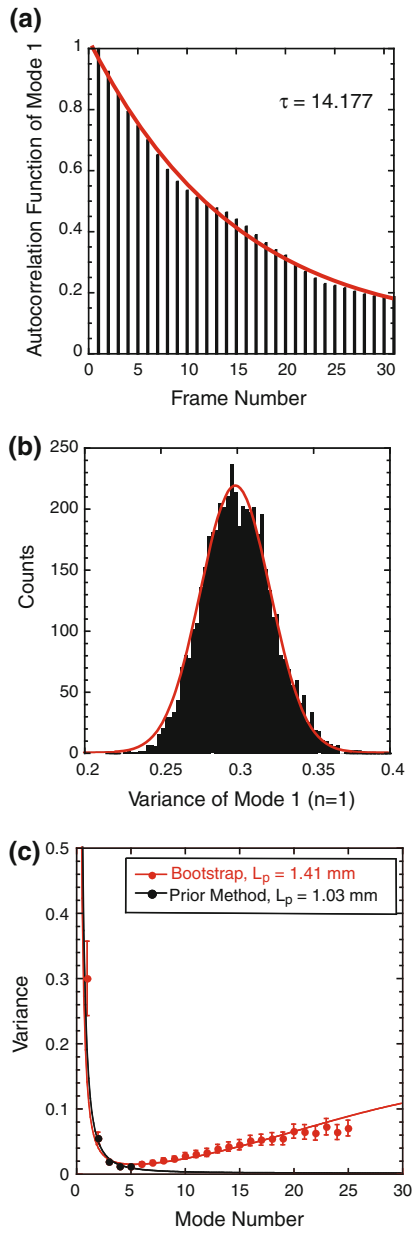

FIGURE 1. Bootstrap analysis of the amplitude data. (a) Plot of the autocorrelation function of the amplitudes of mode 1 (a_1) over time in frames (bars). The data were fit to an exponential decay function: $y(t) = A\exp(-t/\tau_c + B)$, where A is the amplitude, τ_c is the characteristic decay time, and B is a parameter to shift the fit (red line). The value of τ_c determined the number of correlated frames in our raw data. For this example, τ_c = 14.177 frames = 1.418 s. (b) Histogram of the variance of the amplitudes of mode 1 shown in (a) (bars). After bootstrapping 5000 data sets the distribution is normal. The histogram was fit to a Gaussian function to guide the eye (red line). (c) Plot of the variance in pixels as a function of mode number. Red circles indicate the mean variance with error bars representing the standard error calculated from bootstrapping. Black circles plotted for modes 2–5 represent variance calculated from the same data set without bootstrapping as in prior methods. The red curve is a weighted fit of Eq. (1) to all bootstrap data. The black curve is a fit of Eq. (2) to modes 2–5 of the prior method. The persistence length from the bootstrap analysis is 1.41 and 1.03 mm from prior method.

We performed the bootstrap[10] and statistical analysis using R (http://www.R-project.org).[31] Previous reports showed that the amplitude values could be correlated, especially for the first few modes.[2] Therefore, we imported the amplitudes from the MATLAB analysis and applied the auto-correlation function:

$$\mathrm{ACF}_n(\tau) = \frac{\sum_{t=1}^{N_{\max}-\tau} (a_n(t) - \langle a_n \rangle)(a_n(t+\tau) - \langle a_n \rangle)}{\sum_{t=1}^{N_{\max}} (a_n(t) - \langle a_n \rangle)^2} \tag{3}$$

where t is the time step in frames, τ is the frame shift of the correlation, $N_{\max}$ is the maximum number of frames, and $\langle a_n \rangle$ denotes the average value of the nth amplitude (Fig. 1a). We fit the autocorrelation function to a decaying exponential to find the characteristic time of correlation in our data, τ_c. We took the total number of frames, $N_{\max}$, and divided it by the correlation time to determine the number of independent frames, N_{ind}. We adopted a subsampling bootstrap technique[30] where we randomly sampled N_{ind} frames from our data set. This approach is suitable since there is not a unique set or selection of "independent" frames, and, due to the stochastic dynamics, independent frames are not simply evenly spaced in the data set. By resampling the data and calculating the distribution of our statistic (in this case Fourier coefficients), we obtain a better estimate for the statistic as well as its standard error.

We sampled with replacement N_{ind} amplitudes from the total of $N_{\max}$ frames, calculating the variance for each mode and repeating this procedure 5000 times. A histogram of the 5000 variances showed a normal distribution (Fig. 1b), as expected. We directly calculated the mean variance as well as its standard error. We plotted the variance with error as a function of the mode number and fit the first 25 modes using weighted multiple linear regression to find the parameters, L_p and $\langle \varepsilon_k^2 \rangle$ in Eq. (1) (Fig. 1c, red circles and red fit curve). The weighting was done using the inverse of the standard error of each point. The errors in the fits for L_p and $\langle \varepsilon_k^2 \rangle$ were quoted as the error for each.

RESULTS

Bootstrapping to Find an Error in the Variance

Previous measurements that have used freely fluctuating cytoskeletal filaments calculated the variance in the normal modes to determine the persistence length of the filament, using Eq. (1). This method is correct in practice, however it is prone to error since it is strongly dependent on the variance of the first few modes, and these modes have potential inaccuracies due to sampling and correlation issues.

To overcome this problem, one could determine the error in the variance directly by sampling the same microtubule multiple times. Unfortunately, the illumination causes photobleaching that decreases signal. Further, photodamage will likely alter the microtubule properties over the time it would take to collect the data. Instead, we decided to use bootstrapping to resample the mode amplitudes. We first determined the number of independent frames, N_{ind}, by finding the autocorrelation time for the first Fourier mode (Fig. 1a). We then sampled N_{ind} frames out of the full data set, with replacement, and then calculated the variance for each mode. By repeating this resampling procedure 5000 times, we recovered a normal distribution (Fig. 1b) allowing us to assign a mean variance as well as a standard error for each mode. These values were used to perform a weighted multiple linear regression using Eq. (1) to determine the values for L_{p} and $\langle \varepsilon_k^2 \rangle$ (Fig. 1c).

Our bootstrapping of the amplitude data gave us more information about the variance of the data, which allowed us to place error bars and perform a weighted fit of Eq. (1) to the variance as a function of mode number (Fig. 1c). When the fit to variance data for all 25 modes was performed without weighting, we found the noise regime alters the fit of Eq. (1) resulting in a persistence length that is 3 orders of magnitude lower than expected (Supplemental data, Fig. 1A). It is clear from the plot that the fit to the low modes is suffering to accommodate the higher mode fit. Thus, in order to use Eq. (1) to fit all data, weighting was required. This poor fitting of Eq. (1) to all the mode data is why prior groups used the shorter Eq. (2) to fit to just the lowest few modes.[13]

We deduced the persistence length from our unweighted, low mode data using Eq. (2) and compared it to the persistence length determined from our weighted data over all modes using Eq. (1). We noticed that there was a slight increase in the resulting persistence length using the weighted fit (Fig. 1c, Supplemental Fig. 1B). The bootstrapping did not change the variance of the mode measurements by very much, so this cannot account for the differences in measured persistence length for the prior and bootstrapping methods. The difference must be accounted for in the fitting of the data. We believe that the increased persistence lengths determined by the weighted fit are a better estimate of the true persistence lengths because they take experimental error into account.

Persistence Length is a Log-Normal Distribution

We measured the persistence length of over 200 microtubules with a variety of different conditions. For any one condition, we found that a histogram of the persistence length is log-normally distributed (Fig. 2a). Log-normal distributions are characterized by a smaller median value than the mean and a long tail at larger values. We fit our data to a log-normal function:

$$f(x) = A \exp\left(-\frac{(\ln(x - x_0))^2}{2S^2} \right) \tag{4}$$

where A is the amplitude of the function, x_0 is the center of the distribution, and S relates to the width (Chi-squared = 212). Log-normal distributions are usually the result if the variable is a product of independent variables with similar widths.[22] The persistence length is a product of the Young's Modulus (E) and the 2nd moment of area (I) divided by the product of the Boltzmann constant (k_{B}) and absolute temperature (T):

$$L_{\text{p}} = \frac{EI}{k_{\text{B}}T} \tag{5}$$

where (E) and (I) are both likely normally distributed about their average values for real microtubules (see "Discussion" section).

We transformed the data by performing the natural log operation and found that the transformed data were Gaussian, as expected for log-normal data (Fig. 2b, fit parameters in the caption, Chi-squared = 0.003). We performed the binning with several bin sizes, and found they all showed a normal distribution with similar fit parameters. In order to compare persistence length data between different conditions and prove that they are statistically significant, we compared histograms of the ln-transformed data because they are normally distributed.

Another method to compare probability distributions is to compare the cumulative distributions. Cumulative distributions do not require binning the data and the possible errors that can arise through that process. We normalized the cumulative distributions so that the total cumulative probability for all microtubules equaled one. We will compare normalized cumulative probability distributions between different data sets to demonstrate that different conditions are distinct.

Persistence Length Depends on Tubulin Preparation

We polymerized microtubules from two different preparations of tubulin and consistently found different persistence lengths distributions depending on the tubulin preparation method (Fig. 3a). The PC purified, lyophilized tubulin was purchased from Cytoskeleton, called "commercial." We also prepared tubulin in house by removing MAPs with a high concentration of PIPES salts, called "in-house." Each of these batches consistently showed the same persistence length

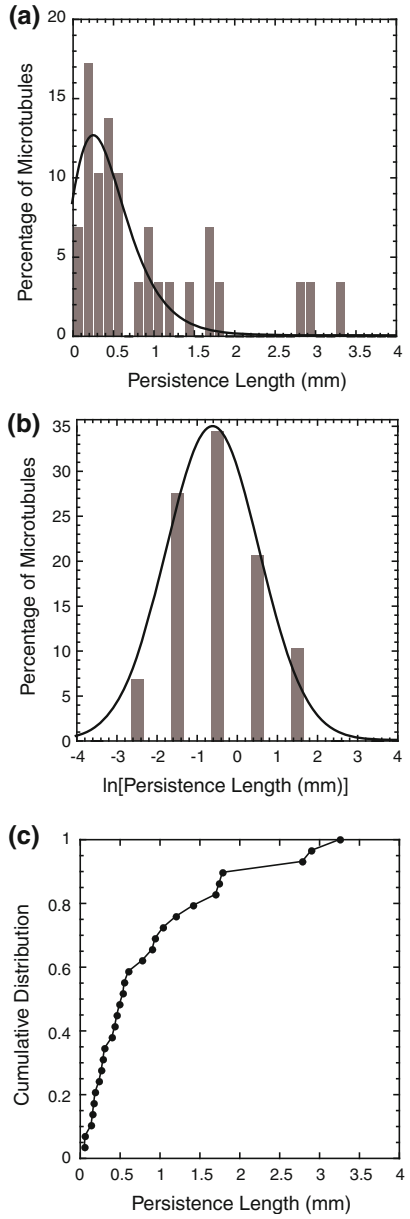

FIGURE 2. Distribution of the persistence length data were log-normal. (a) Normalized histogram of the microtubule persistence length (bars) fit to a log-normal function, Eq. (4) (line). Fit parameters for the data are $A = 12 \pm 2$, $x_0 = -0.73 \pm 0.07$, $S = 0.33 \pm 0.06$, and the goodness of fit is 0.66, the Chi-squared is 212, and the number of microtubules is 29. (b) Normalized histogram of the natural ln-transformed persistence length (bars) fit to a normal, Gaussian distribution (line). Fit parameters for the data are $A = 35 \pm 2$, $x_0 = -0.59 \pm 0.08$, $\sigma = 1.6 \pm 0.1$, and the goodness of fit is 0.98, the Chi-squared is 0.003, and the number of microtubules is 29. (c) Cumulative distribution of persistence length. The cumulative distribution was found by the following procedure: The persistence lengths were arranged in ascending order. We numbered the persistence length values from 1 to *n*, where *n* is the number of microtubules in the sample, in order to sum the number of microtubules with persistence length at or below the given value. We normalized the cumulative distribution by dividing the series 1 to *n* by *n*, so that the total probability of finding a persistence length of the maximum value or lower was equal to one.

distribution for multiple aliquots of the same tubulin. To compare these two types, we kept the rhodamine concentration at 16% and measured them within 3–6 h of polymerization. We find that the commercial tubulin is stiffer ($L_p = 1.6 \pm 0.3$ mm, fit parameters given in the figure caption, Chi-squared = 0.003) than the in-house tubulin ($L_p = 0.6 \pm 0.1$ mm, fit parameters given in the figure caption, Chi-squared = 0.003) (Fig. 3a). We performed a student's *t*-test on the distributions of ln-transformed data and found there is only a 0.1% probability that these distributions are the same. Therefore, we are 99.9% confident that these distributions are distinct. These differences are also illustrated in the cumulative probability distributions (Fig. 3b).

We performed SDS-Page gels with Coomassie blue staining to quantify the percentage of contaminating MAPs in each preparation. We loaded wells with 20, 10, or 5 μg of tubulin dimers from the commercial or in-house tubulin. We quantified the intensity of each band using ImageJ. We found that both the in-house and commercial tubulin were about 99% pure tubulin with only a few contaminating bands in the high molecular weight range >100 kD (Supplemental Fig. 2B).

Using SDS-Page alone, we cannot tell if these contaminating bands are MAPs or other proteins that do not bind to microtubules. In order to test if these proteins consisted of functional MAPs, we ran SDS-Page gels of the polymerized microtubules we used in our samples after the final pelleting step. Interestingly, the high molecular weight bands of the tubulin samples are enhanced in the commercial samples after polymerizing and pelleting (Fig. 3c). The fact that these high molecular weight proteins are present after pelleting means that they were bound to the microtubules, and they are likely MAPs. The darkening of these bands after pelleting means that the concentration has increased slightly compared to the concentration in the tubulin dimer sample (compare Supplemental Fig. 2B with Fig. 3c). This corroborates the conclusion that they are active MAPs. We do not see this enhancement of the bands in the in-house tubulin samples (compare Supplemental Fig. 2B with Fig. 3c).

Persistence Length Changes with Age

For each type of preparation, commercial and in-house tubulin, we performed assays on the same Taxol-stabilized microtubules within 3–6 h of polymerization (called "4 h") and then repeated the measurement on the same set of microtubules 24–26 h later (called "24 h"). We repeated these assays on multiple samples of microtubules. All microtubules used 16% rhodamine. We found that the commercial tubulin showed a decrease in average persistence length from 1.6 ± 0.2 mm to 0.8 ± 0.1 mm after 24 h (Fig. 4a, fit

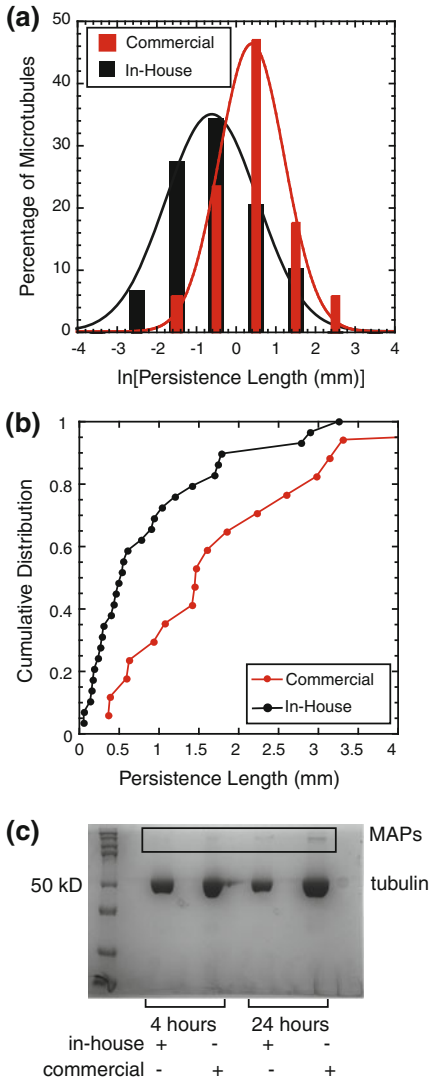

FIGURE 3. Microtubule persistence length depends on preparation. (a) Normalized histograms of natural log-transformed microtubule persistence length with fits to Gaussian functions for measurements made from commercial tubulin (red bars, red line) or in-house tubulin (black bar, black line). Fit parameters for the commercial tubulin data are $A = 46 \pm 2$, $x_0 = 0.41 \pm 0.05$, $\sigma = 1.16 \pm 0.07$, and the goodness of fit is 0.98, the Chi-squared is 0.003, and the number of microtubules is 17. Fit parameters for the in-house tubulin data are $A = 35 \pm 2$, $x_0 = 0.59 \pm 0.08$, $\sigma = 1.6 \pm 0.1$, and the goodness of fit is 0.98, the Chi-squared is 0.003, and the number of microtubules is 29. (b) The cumulative distribution of microtubule persistence length for commercial tubulin (red circles, red line) and in-house tubulin (black circles, black line. (c) Coomassie-stained SDS-PAGE protein gel of 10 μg of in-house (lanes 3 and 7) and commercial (lanes 5 and 9) microtubules after polymerization and pelleting, as described for use in the methods. The box denotes the residual high molecular weight proteins. The image has had the brightness and contrast enhanced maintaining a linear scale so that these bands are easier to visualize. Microtubules were collected as samples 4 h (lanes 3 and 5) and 24 h (lanes 7 and 9) after polymerization. Lane 1 shows molecular weight markers of 250, 150, 100, 75, 50, 37, and 25 kD.

parameters given in the figure caption, Chi-squared = 0.003 for 4 h and 0.005 for 24 h data fits). We performed a student's *t*-test on the distributions of ln-transformed data and found only a 0.1% probability that they are the same distribution. Therefore, we are 99.9% confident that the persistence length of the commercial microtubules changed over a one-day time course. The differences are also clear in the cumulative probability distributions (Fig. 4b).

The in-house tubulin had a consistent and lower persistence length over time. On the day of creation, the average persistence length was 0.6 ± 0.1 mm, and 24 h later, the average persistence length was 0.6 ± 0.1 mm (Fig. 4c, fit parameters given in the figure caption, Chi-squared = 0.005 for both 4 and 24 h data fits). We performed a student's *t*-test on the distributions of ln-transformed data, and there is a 74% chance that these are the same distribution. Thus, we conclude that the persistence length does not change for the in-house microtubules. The cumulative probability distributions of the 4 and 24 h data are also very similar. At short persistence lengths, they are virtually identical, but do diverge for persistence lengths longer than 0.6 mm (Fig. 4d). This divergence is also observed in the ln-transformed data histograms (Fig. 4c).

Persistence Length is Independent of Rhodamine Labeling

We measured the persistence length of microtubules made with 7, 10, 16, and 25% rhodamine-labeled tubulin dimers. We measured the persistence length of Taxol-stabilized microtubules at 4 and 24 h. We decided to use the data from 24 h because (1) the data were always more consistent after 24 h, and (2) the commercial tubulin data became the same as the in-house tubulin data after 24 h. We found that the percentage of rhodamine-labeled dimers did not affect the persistence length significantly (Fig. 5). In order to display the probability distribution, we used box-plots that denote the minimum value, maximum value, first, second, and third quartiles. It is clear that these distributions overlap significantly. We also performed the ANOVA test to compare the four distributions and found no statistically significant differences in the distributions ($p = 0.31$). Thus, we conclude that rhodamine labeling does not affect the persistence length measurement.

Persistence Length is Independent of Filament Length for Short Microtubules

Two recent publications have shown that the persistence length of the microtubule is length dependent

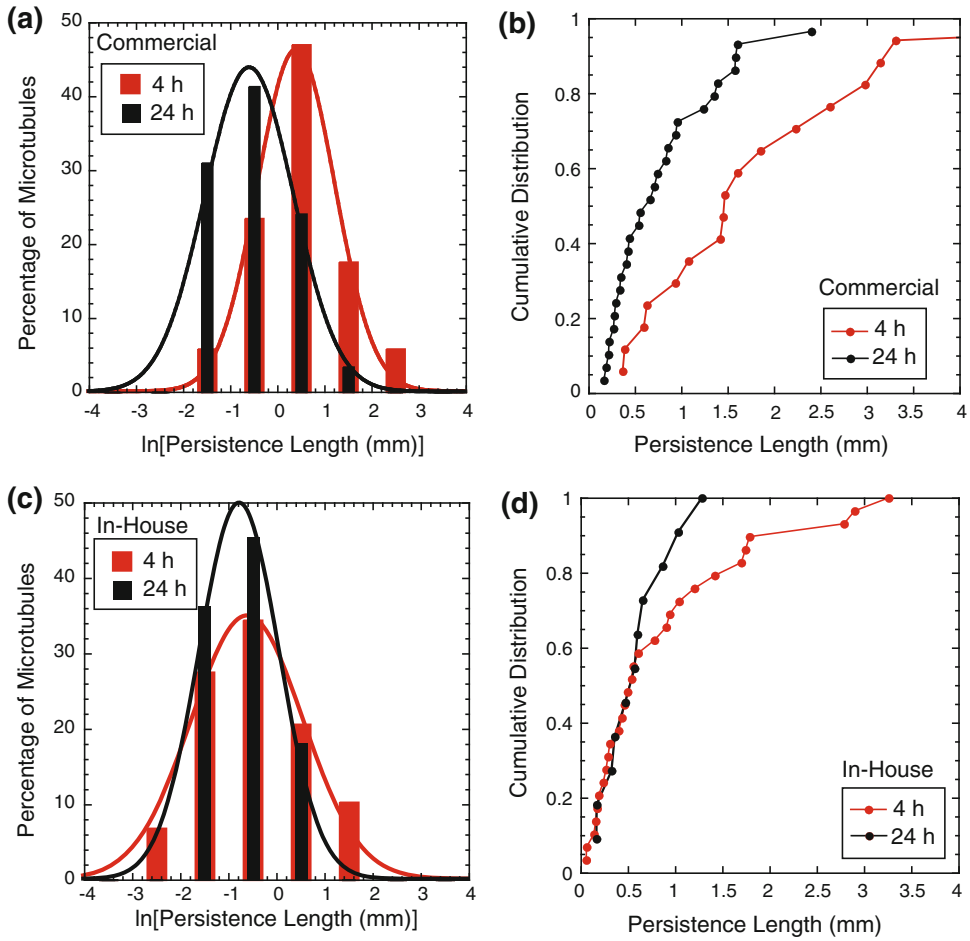

FIGURE 4. Age-dependence of microtubule persistence length depends on preparation. (a) Normalized histograms of natural log-transformed microtubule persistence length with fits to Gaussian functions for measurements of commercial microtubules that are 4 h old (red bars, red line) and 24 h old (black bars, black line). Fit parameters for the 4 h data are $A = 46 \pm 2$, $x_0 = 0.41 \pm 0.05$, $\sigma = 1.16 \pm 0.07$, and the goodness of fit is 0.98, the Chi-squared value is 0.003, and the number of microtubules is 17. Fit parameters for the 24 h data are $A = 44 \pm 3$, $x_0 = -0.59 \pm 0.08$, $\sigma = 1.3 \pm 0.1$, and the goodness of fit is 0.97, the Chi-squared value is 0.005, and the number of microtubules is 29. (b) Cumulative distribution of commercial tubulin persistence length measured at 4 h (red circles, red line) and at 24 h (black circles, black line). (c) Normalized histograms of log-transformed microtubule persistence length with fits to Gaussian functions for measurements of in-house microtubules that are 4 h old (red bars, red line) or 24 h old (black bar, black line). Fit parameters for the 4 h data are $A = 35 \pm 2$, $x_0 = -0.59 \pm 0.08$, $\sigma = 1.6 \pm 0.1$, and the goodness of fit is 0.98, the Chi-squared value is 0.005, and the number of microtubules is 29. Fit parameters for the 24 h data are $A = 50 \pm 3$, $x_0 = -0.76 \pm 0.06$, $\sigma = 1.18 \pm 0.09$, and the goodness of fit is 0.97, the Chi-squared value is 0.005, and the number of microtubules is 11. (d) Cumulative distribution of in-house tubulin persistence length measured at 4 h (red circles, red line) and at 24 h (black circles, black line).

for short microtubules ($5\ \mu m < L_c < 35\ \mu m$).[21,28] Although we do see a number of significant changes to the persistence length as a function of microtubule preparation, we do not see dependence on the contour length in our data. We plotted the persistence length as a function of microtubule contour length for both the prior analysis method and using the bootstrap (Fig. 6b). We see no difference between the two methods, and both are independent of the microtubule contour length for short microtubules. If all of our data were plotted together, it could appear that there is a length-dependent persistence length, but there was a lot of scatter in the data (200 microtubules, Fig. 6a).

DISCUSSION

We have measured the effects of fluorescent labeling, tubulin preparation, and microtubule age on microtubule rigidity. We employed a standard thermal fluctuation method with automated analysis combined with a new bootstrapping method to determine the error in our measurement and to achieve more reliable results. We prefer the bootstrapping method to prior methods for several reasons: (1) It allows us to calculate the error in the variance without repetitious experiments on degrading samples. (2) It allows us to perform a least-squares fit to the variance data for all

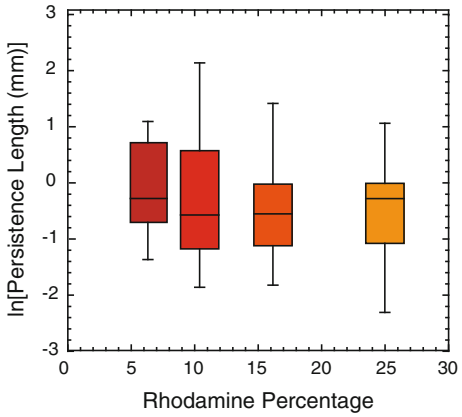

FIGURE 5. Microtubule persistence length does not depend on rhodamine content. Box plots of the log-transformed microtubule persistence length measurements for in-house microtubules measured 24 h after polymerization. We tested four different concentrations of rhodamine, 7% (n = 14, maroon), 10% (n = 20, red), 16% (n = 40, orange) and 25% (n = 31, peach), respectively. The box plot represented the distribution of the data: The minimum is represented by the lower bar; the first quartile (Q1) is represented by the bottom of the box; the median (Q2) is represented by the middle line of the box; the third quartile (Q3) is represented by the top of the box; the maximum value is represented by the upper bar. The median values for 7, 10, 16, 25% are −0.26, −0.56, −0.54, −0.26, respectively.

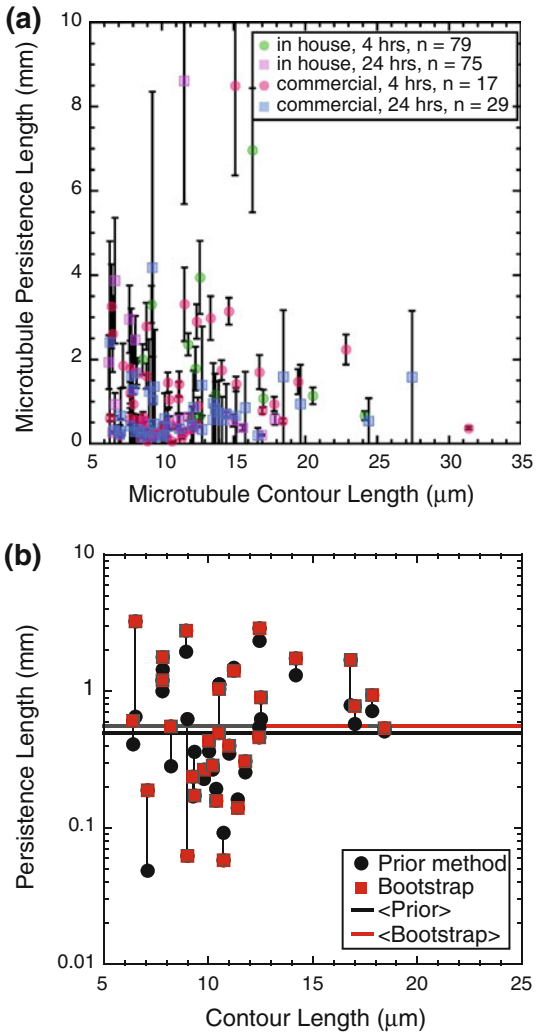

FIGURE 6. Persistence length does not depend on microtubule contour length. (a) We plotted the microtubule persistence length as a function of contour length for 200 microtubules measured with different conditions. We combined the different rhodamine-labeling conditions together to show the data for in-house microtubules at 4 h (green circles), in-house microtubule at 24 h (purple squares), commercial microtubules at 4 h (pink circle), and commercial microtubules at 24 h (blue squares). (b) Plot of the persistence length of microtubules (y-axis) for both the prior method (black circles) and the bootstrap method (red squares) plotted against the microtubule contour length (x-axis). We see no dependence of the persistence length on the contour length for either method. Mean values are denoted by horizontal lines for prior (black line) and bootstrap (red line) methods.

the modes, instead of taking only the first few modes into account, as previous groups have done. (3) We perform the fitting of Eq. (1) to our data in a smart way by taking the error into account, thus the fit uses all the data, but fits to the low-noise regime better. Further, we find that the bootstrapping method and weighted fitting results in lower error in the determined persistence length, which gives us more confidence in our comparisons between different conditions (Supplemental Fig. 1C). It should be noted that, as this paper was under review, another method using spectral analysis was published and had fundamentally similar results in terms of determining the error of the variance to allow a global fit to all the mode data.[35] Using this method, the results obtained for Taxol-stabilized microtubules were similar to ours.

Although the persistence length has been measured before, no previous study has examined the distribution of the persistence length or tried to understand why there is such a high variability in the measurement. We find that the distribution is log-normal, and that solid statistics can be done with distributions of ln-transformed data, allowing unambiguous comparisons between different experimental states. The log-normal distribution was also reported in a very recent publication where they use a spectral analysis method to perform the measurements only on Taxol-stabilized microtubules.[35] This group does not describe why there is a log-normal distribution. We believe that the large variability and the log-normal nature of the distribution are due to the inhomogeneities in the microtubule population used in the assays. We are using Taxol-stabilized microtubules, which are known to have a variable protofilament number and helicity and dislocation defects, or protofilament shifts, within individual microtubules.[1,5] Although we typically assume that I, is constant, several structural studies have shown that Taxol-stabilized microtubules can

have protofilament numbers from 12 to 15.[6] From cross-sectional images of these microtubules, we have estimated that I ranges from $I_2 = 6.7 \times 10^3$ to $I_{15} = 2.8 \times 10^4$ nm^4. Further, several studies have demonstrated that Taxol-stabilized microtubules (stabilized with Taxol 1 day after polymerization) have a protofilament shift defect along their lengths, at a frequency of 1 defect per 15–17 μm.[1,5] Although we stabilized with Taxol immediately after polymerization in the absence of Taxol, we believe these Taxol-stabilized microtubules will still have more defects than microtubules without Taxol. The defects will effectively broaden the distribution of I even for a single microtubule. Finally, in addition to actual size changes, the microtubule cross-section has been shown to fluctuate in shape from circular to oval in high-resolution structural studies,[6] and these fluctuations could also contribute to changes in I.

We have shown that there is a difference in the persistence length by a factor of two depending on the preparation. We compared commercially available PC tubulin to our in-house tubulin. Both preparations remove MAPs using ionic strength, but do so by different methods. Both preparations result in relatively clean tubulin 99% pure with a few contaminating proteins of high molecular weight (Fig. 3c, Supplemental Fig. 2B). We find that the contaminating bands of the commercial tubulin represent active MAPs that could be binding and enhancing the rigidity of the microtubules. It has been shown that structural MAPs, such as tau and MAP2, can increase the persistence length of microtubules.[9,11,23] One study examined the effects of both Taxol and increasing concentrations of full-length tau protein, a MAP that enhances growth and stability of microtubules in axons.[11] First, they established that Taxol-stabilized microtubules had a persistence length of 0.2 mm, similar to our measurements. Further, they found that tau enhanced the persistence length proportional to the concentration of tau present. For instance, 2% tau (ratio compared to tubulin dimer content) increased the persistence length from 0.9 ± 0.2 mm (without Taxol) 1.1 ± 0.4 mm, and 18% tau increased the persistence length to 2.2 ± 0.3 mm. They also found that MAP2, a dendritic stabilizing MAP, increased the persistence length even more than tau, and a brain MAP-mix was even more potent. Interestingly, Dye *et al.*[9] found that microtubules with MAP2 and Taxol together had the same flexibility as MAP2 alone, implying that the increased flexibility of Taxol and the increased rigidity of MAP2 do not cancel each other out. We do not know exactly which brain MAPs are residual in the commercial or in-house preparations, but they may contribute to the increased the persistence length we observe.

We have presented evidence that seemingly minor alterations to the preparation of microtubules can have a qualitative (factor of 2) effect on the resulting persistence length measured. This effect is consistent and statistically significant, but does not capture the two orders of magnitude discrepancy in measured values in the literature (for a comprehensive review with table of prior measurements, see Hawkins *et al.*[15]). If one compares the measured flexural rigidities for Taxol-stabilized microtubules measured by a variety of means, there is as much variance for the 22 reported measurements as there are in our single set of measured microtubules ($n = 200$). These measurements have been made with different techniques (freely fluctuating filaments with one or both ends free, calibrated flow, buckling with optical traps, buckling with kinesin motors, and forced bending against viscous drag), but the data have similar results from wildly different techniques, and wildly different results from the same technique. Perhaps, the variation derives not only from the effects we observe in preparation, but also in different values for the second moment of inertia, and the low numbers of measurements for performing the required statistical analyses needed. Our data sit in the middle of the range of data collected from other groups. Given the high and asymmetric variance of the data, we propose that higher number of microtubules need to be measured and histograms of the results must be used to compare differences in future studies.

One might expect that, as the dimers begin to degrade, the microtubules would become more flexible over time. We kept the same stock preparation of polymerized microtubules at 37 °C over 24 h to examine the same set of microtubules directly after polymerization and then 1 day later. We found that age had large effect for the commercial tubulin preparation and not for the in-house preparation (Figs. 4a, 4b). We find that after 24 h of incubation, the persistence length of the commercial microtubules drops to the same level as the in-house microtubules, which is constant over 24 h (Fig. 4c, Supplemental Fig. 2A). One possible explanation for this aging effect could be that the residual contaminating MAPs present in the commercial tubulin lose activity after 24 h. Another possible explanation is that the more rigid microtubules are less stable and disassemble after 24 h, or that the microtubules end-to-end anneal so that the entire population is more homogeneous and flexible.

We tested the effect of increasing the number of rhodamine-labeled tubulin dimers in the microtubule, and found it has no effect. Rhodamine-labeling consists of covalently linking a rhodamine dye to surface lysine residues of the tubulin dimer. Lysines are found around the surface, but predominantly at the inter-dimer interfaces. The labeling is performed on

polymerized microtubules to reduce the labeling on the lysines essential for polymerization. Despite this care, up to 90% of tubulin dimers are lost and unable to repolymerize in the labeling process, implying that those lysines are labeled and affect polymerization.[18] Our results indicate that the remaining 10% of labeled dimers are probably labeled on lysines outside of the inter-dimer regions, because we see no change in persistence length with increasing concentrations of labeled dimers. This compliments some recent work performed on the polymerization kinetics of labeled microtubules where they also find that high levels of labeled tubulin dimers do not affect the dynamics of microtubules.[12]

Measurements of microtubule persistence length inside cells are difficult because we cannot quantify the forces acting along the microtubule. Unlike in our simple, thermally driven *in vitro* system, the forces inside cells include active motors and confining forces due to other filaments. Microtubules inside cells have been observed to create high curvature.[25] Sometimes they break and sometimes they do not. We have shown that much of the breakage is due specifically to the activity of microtubule-severing enzymes.[37] After breakage, the microtubules can retain their curvature, implying that the forces acting on them persist.[36] One possible means to determining the persistence length of cellular microtubules would be to gently extract intact microtubules from cells with their bound MAPs, but removing the crowding and crosslinking active agents. Using these extracted microtubules in a thermal experimental system would allow for measurements of natural microtubules with all the intact isotypes, post-translational modifications, and MAPs. If successful, such experiments could also compare between microtubule populations in different cell types and compartments, such as axons and dendrites.

CONCLUSIONS

Microtubule persistence length has been measured numerous times over the years with varying results for similar experimental systems. Here, we have presented results that through meticulous experiments and statistical analysis, clear conclusions can be made about the persistence length of microtubules, and how even something as innocuous as different preparations of tubulin can greatly affect the measurement by a factor of 2. The measurements made over the years have the same variation in the results that a single measurement of many microtubules has, implying that this measurement is tricky and requires high repetitions and careful analysis. Using an improved bootstrapping analysis to estimate the error of the variance, we can now begin to compare data for microtubules of different conditions, such as tubulin isotype, post-translational modification, or species-dependent effects. Further, MAPs that both increase or decrease the rigidity need to be explored.

ELECTRONIC SUPPLEMENTARY MATERIAL

The online version of this article (doi:10.1007/s12195-012-0229-8) contains supplementary material, which is available to authorized users.

ACKNOWLEDGMENTS

TLH was supported in part from the North East Alliance for Graduate Education and Professoriate (NEAGEP) grant from the NSF. TLH, MM, and MSY were supported on an NSF grant #1039403 and supplement #0928540 to JLR and DS from the Nano and Bio Mechanics Program, Civil Mechanical, and Manufacturing Innovation Directorate. DLS was supported by funds from the Intramural Research Program of the Eunice Kennedy Shriver National Institute of Child Health and Human Development. We thank Carey Fagerstrom for her preparation of the in-house tubulin and helpful discussions. We thank John Crocker for valuable discussions on statistics and log-normal data sets.

REFERENCES

[1]Arnal, I., and R. H. Wade. How does taxol stabilize microtubules? *Curr. Biol.* 5:900–908, 1995.
[2]Brangwynne, C. P., G. H. Koenderink, E. Barry, Z. Dogic, F. C. MacKintosh, and D. A. Weitz. Bending dynamics of fluctuating biopolymers probed by automated high-resolution filament tracking. *Biophys. J.* 93:346–359, 2007.
[3]Brown, T. B., and W. O. Hancock. A polarized microtubule array for kinesin-powered nanoscale assembly and force generation. *Nano Lett.* 2:1131–1135, 2002.
[4]Cassimeris, L., D. Gard, P. T. Tran, and H. P. Erickson. XMAP215 is a long thin molecule that does not increase microtubule stiffness. *J. Cell Sci.* 114:3025–3033, 2001.
[5]Chrétien, D., F. Metoz, F. Verde, E. Karsenti, and R. H. Wade. Lattice defects in microtubules: protofilament numbers vary within individual microtubules. *J. Cell Biol.* 117:1031–1040, 1992.
[6]Chrétien, D., and R. H. Wade. New data on the microtubule surface lattice. *Biol. Cell* 71:161–174, 1991.
[7]Clemmens, J., H. Hess, R. Doot, C. M. Matzke, G. D. Bachand, and V. Vogel. Motor-protein "roundabouts": microtubules moving on kinesin-coated tracks through engineered networks. *Lab Chip* 4:83–86, 2004.
[8]Desai, A., and T. J. Mitchison. Microtubule polymerization dynamics. *Annu. Rev. Cell Dev. Biol.* 13:83–117, 1997.

[9]Dye, R. B., S. P. Fink, and R. C. Williams. Taxol-induced flexibility of microtubules and its reversal by MAP-2 and Tau. *J. Biol. Chem.* 268:6847–6850, 1993.
[10]Efron, B., and R. Tibshirani. An Introduction to the Bootstrap. New York: Chapman and Hall, 1993.
[11]Felgner, H., R. Frank, J. Biernat, E. M. Mandelkow, E. Mandelkow, B. Ludin, A. Matus, and M. Schliwa. Domains of neuronal microtubule-associated proteins and flexural rigidity of microtubules. *J. Cell Biol.* 138:1067–1075, 1997.
[12]Gardner, M. K., B. D. Charlebois, I. M. Jánosi, J. Howard, A. J. Hunt, and D. J. Odde. Rapid microtubule self-assembly kinetics. *Cell* 146:582–592, 2011.
[13]Gittes, F. Flexural rigidity of microtubules and actin filaments measured from thermal fluctuations in shape. *J. Cell Biol.* 120:923–934, 1993.
[14]Goel, A., and V. Vogel. Harnessing biological motors to engineer systems for nanoscale transport and assembly. *Nat. Nanotechnol.* 3:465–475, 2008.
[15]Hawkins, T., M. Mirigian, M. Selcuk Yasar, and J. L. Ross. Mechanics of microtubules. *J. Biomech.* 43:23–30, 2010.
[16]Hess, S. T., T. P. Girirajan, and M. D. Mason. Ultra-high resolution imaging by fluorescence photoactivation localization microscopy. *Biophys. J.* 91:4258–4272, 2006.
[17]Hutchins, B. M., M. Platt, W. O. Hancock, and M. E. Williams. Directing transport of $CoFe_2O_4$-functionalized microtubules with magnetic fields. *Small* 3:126–131, 2007.
[18]Hyman, A., D. Drechsel, D. Kellogg, S. Salser, K. Sawin, P. Steffen, L. Wordeman, and T. Mitchison. Preparation of modified tubulins. *Methods Enzymol.* 196:478–485, 1991.
[19]Janson, M. E., and M. Dogterom. A bending mode analysis for growing microtubules: evidence for a velocity-dependent rigidity. *Biophys. J.* 87:2723–2736, 2004.
[20]Kawaguchi, K., S. Ishiwata, and T. Yamashita. Temperature dependence of the flexural rigidity of single microtubules. *Biochem. Biophys. Res. Commun.* 366:637–642, 2008.
[21]Kawaguchi, K., and A. Yamaguchi. Temperature dependence rigidity of non-taxol stabilized single microtubules. *Biochem. Biophys. Res. Commun.* 402:66–69, 2010.
[22]Limpert, E., W. A. Stahel, and M. Abbt. Log-normal distributions across the sciences: keys and clues. *Bioscience* 51:341–352, 2001.
[23]Mickey, B., and J. Howard. Rigidity of microtubules is increased by stabilizing agents. *J. Cell Biol.* 130:909–917, 1995.
[24]Nitta, T., and H. Hess. Dispersion in active transport by kinesin-powered molecular shuttles. *Nano Lett.* 5:1337–1342, 2005.
[25]Odde, D. J., L. Ma, A. H. Briggs, A. DeMarco, and M. W. Kirschner. Microtubule bending and breaking in living fibroblast cells. *J. Cell Sci.* 112(Pt 19):3283–3288, 1999.
[26]Ott, A., M. Magnasco, A. Simon, and A. Libchaber. Measurement of the persistence length of polymerized actin using fluorescence microscopy. *Phys. Rev. E Stat. Phys. Plasmas Fluids Relat. Interdiscip. Topics* 48:R1642–R1645, 1993.
[27]Pampaloni, F., and E. L. Florin. Microtubule architecture: inspiration for novel carbon nanotube-based biomimetic materials. *Trends Biotechnol.* 26:302–310, 2008.
[28]Pampaloni, F., G. Lattanzi, A. Jonás, T. Surrey, E. Frey, and E. L. Florin. Thermal fluctuations of grafted microtubules provide evidence of a length-dependent persistence length. *Proc. Natl Acad. Sci. USA* 103:10248–10253, 2006.
[29]Peloquin, J., Y. Komarova, and G. Borisy. Conjugation of fluorophores to tubulin. *Nat. Methods* 2:299–303, 2005.
[30]Politis, D. N., and J. P. Romano. Subsampling. New York: Springer, 1999.
[31]R Development Code Team. R Code, 2011.
[32]Raviv, U., T. Nguyen, R. Ghafouri, D. J. Needleman, Y. Li, H. P. Miller, L. Wilson, R. F. Bruinsma, and C. R. Safinya. Microtubule protofilament number is modulated in a stepwise fashion by the charge density of an enveloping layer. *Biophys. J.* 92:278–287, 2007.
[33]Shelanski, M. L., F. Gaskin, and C. R. Cantor. Microtubule assembly in the absence of added nucleotides. *Proc. Natl Acad. Sci. USA* 70:765–768, 1973.
[34]Taute, K. M., F. Pampaloni, E. Frey, and E. L. Florin. Microtubule dynamics depart from the wormlike chain model. *Phys. Rev. Lett.* 100:028102, 2008.
[35]Valdman, D., P. J. Atzberger, D. Yu, S. Kuei, and M. T. Valentine. Spectral analysis methods for the robust measurement of the flexural rigidity of biopolymers. *Biophys. J.* 102:1144–1153, 2012.
[36]Wakida, N. M., C. S. Lee, E. T. Botvinick, L. Z. Shi, A. Dvornikov, and M. W. Berns. Laser nanosurgery of single microtubules reveals location-dependent depolymerization rates. *J. Biomed. Opt.* 12:024022, 2007.
[37]Zhang, D., K. D. Grode, S. F. Stewman, J. D. Diaz-Valencia, E. Liebling, U. Rath, T. Riera, J. D. Currie, D. W. Buster, A. B. Asenjo, H. J. Sosa, J. L. Ross, A. Ma, S. L. Rogers, and D. J. Sharp. Drosophila katanin is a microtubule depolymerase that regulates cortical-microtubule plus-end interactions and cell migration. *Nat. Cell Biol.* 13:361–370, 2011.